7th Int. Symp. "Nanostructures: Physics and Technology"
St Petersburg, Russia, June 14–18, 1999

Wide-miniband superlattice devices for microwave and terahertz frequencies

K. F. Renk
Institut für Angewandte Physik, Universität Regensburg, Germany

Abstract. Wide-miniband superlattice devices are suitable for generation, detection and frequency multiplication of microwaves and for detection and autocorrelation of THz radiation. The devices, operated at room temperature, are based on nonlinear transport properties of the miniband electrons. While the interaction of the miniband electrons with microwaves can be described by the nonlinear current-voltage characteristic, interaction with a THz field is based on a quantum nonlinearity, namely a THz-field induced modulation of the Bloch oscillations of the miniband electrons.

Introduction

The devices are the result of a most successful international cooperation, with four partners, A. Ignatov *et al.* (Nizhni Novgorod) delivering the theoretical basis, P. Kop'ev and V. Ustinov *et al.* (St. Petersburg) providing the MBE growth technique, Pawel'ev *et al.* (Nizhni Novgorod) contributing high-frequency device expertise, and E. Schomburg *et al.* (Regensburg) providing high-frequency and THz experience. The work is based on the ideas of Esaki and Tsu [ ], who predicted that semiconductor superlattices should show nonlinear current transport, because of Bloch oscillations [ ] of the miniband electrons. With respect to current transport, especially at high current density, transport properties of doped superlattices have been studied by Sibille and Palmier *et al.* [ ].

1 Negative differential conductance

First, we consider a superlattice (Fig. 1) of 120 periods each period consisting of 49 Å thick GaAs and 13 Å thick AlAs layers, corresponding to a lowest-miniband width of 22 meV. The superlattice (length 0.74 μm) is homogeneously n doped (1.4×10^{17} cm^{-3}) and is embedded in graded layers and n^+ GaAs layers, grown on a n^+ GaAs substrate. A Au-Ge-Ni layer serves as ohmic contact. The superlattice is mesa structured, with a small-area mesa (dimension 7×8 μm) and a large-area mesa (100×200 μm). In this quasi planar device, with two ohmic contacts in one plane, the small-area mesa is the active device while the large-area mesa is a series resistance.

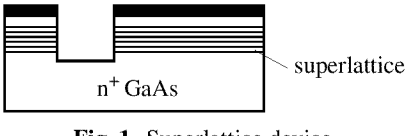

Fig. 1. Superlattice device.

Characteristic for a wide-miniband superlattice is the ability of the miniband electrons to perform Bloch oscillations (Fig. 2). An electron traverses several periods of the superlattice, oscillating back and forth along the superlattice axis, z, being Bragg reflected at the upper

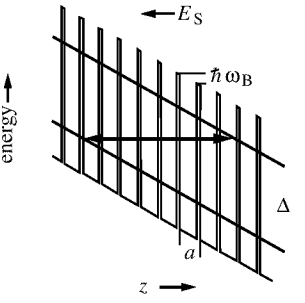

Fig. 2. Bloch oscillation.

boundary of the miniband (width Δ). The oscillation frequency corresponds to the Bloch frequency

$$\omega_B = \frac{ea}{\hbar} E_s \tag{1}$$

where e is the elementary charge, $\hbar$ Planck's constant, a the superlattice period, and E_s the strength of a static electric field along z. The duration of a Bloch oscillation of a miniband electron is limited by the intraminiband relaxation. The Bloch oscillation corresponds to a quantum coherent oscillation within a range of several superlattice periods. After relaxation the coherence is lost and the electron begins a new oscillation. All miniband electrons perform, independently, i. e. without a phase relation to each other, Bloch oscillations.

The current (I)–voltage (U) characteristic of the superlattice (Fig. 3) shows ohmic behavior at small voltage and a negative differential conductance above a critical voltage U_c ($\sim$ 1 V). At the critical voltage an electron performs in the average one Bloch oscillation cycle within the relaxation time ($\tau\omega_B = 1$); the critical voltage corresponds to a Bloch frequency $\omega_B/2\pi = 1.6$ THz and the relaxation time τ is $\sim 10^{-13}$s. Overdamped Bloch oscillations ($\omega_B\tau < 1$) are responsible for the deviation of the current-voltage characteristic from ohmic behavior for voltages $U < U_c$. At $U > U_c$ ($\omega_B\tau > 1$) the increasing number of Bloch oscillation cycles within the relaxation time τ reduces the mean path of a miniband electron and therefore the drift velocity, v_d. The drift velocity-field characteristic is given, for a simple tight binding energy dispersion relation for the miniband, by [ ]

$$v_d = \frac{ea\Delta}{4\hbar} \frac{2\omega_B\tau}{1+\omega_B^2\tau^2}. \tag{2}$$

The peak drift velocity, $v_p = ea\Delta/4\hbar$, increases linearly with Δ. A more elaborated analysis taking into account the thermal distribution of the electrons in the miniband and, furthermore, elastic scattering, delivers the same inelastic intraminiband relaxation time (10^{-13} s) as the simple analysis and an elastic scattering rate of the same order [4]; the inelastic scattering is due to interaction with longitudinal optical phonons and the elastic scattering mainly due to scattering at the GaAs/AlAs interfaces because of roughness. The jumps in the $I-U$ characteristic (Fig. 3) are the consequence of travelling high-field domains. These are the origin of a current oscillation and of microwave generation [3, 4]. The corresponding charge density is a travelling dipole domain, with a depletion layer followed by an accumulation layer, both extending along the superlattice axis over many superlattice periods.

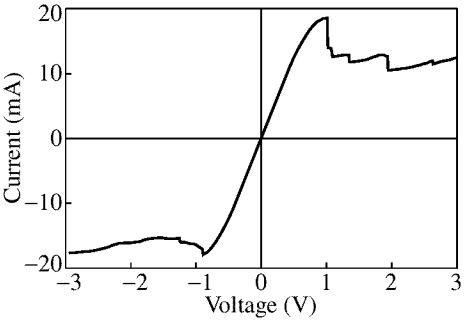

Fig. 3. Current-voltage characteristic.

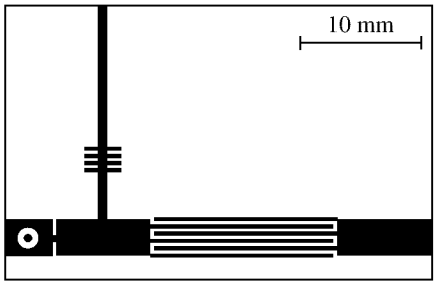

Fig. 4. Superlattice oscillator.

2 Superlattice oscillator

A superlattice device (with the data given in section 1) was integrated into a planar circuit (Fig. 4) with a low-pass port for the direct current supplied by a constant-voltage source, and a high-pass port for the microwaves [9].

The oscillator showed an emission spectrum (Fig. 5) with a fundamental harmonic near 5 GHz and higher harmonics. The fundamental frequency ν_{osc} was equal to the inverse superlattice transit time of the dipole domains, which travelled with a velocity near the peak drift velocity. The occurrence of higher harmonics indicates that the domains had an extension which was shorter than the superlattice length. The power of the oscillator was 1 mW (efficiency 6%).

A weak narrow-band external field is able to phaselock the oscillator [9]. Instead of a bandwidth of about 1 MHz the locked superlattice oscillator now has a bandwidth,

which is comparable with the linewidth ot the external field (e.g. 10 Hz); the locking leads to a suppression of thermal fluctuations occurring in the formation of the domains.

Superlattices with wider minibands show (at comparable superlattice length L) larger fundamental frequencies (Fig. 6). The frequency of the oscillation corresponds to the ratio of the domain velocity and the superlattice length and is approximately given by $\nu_{\mathrm{osc}} \sim 0.7 v_{\mathrm{p}}/L$ [4, 8]. Recently, a GaAs/AlAs superlattice oscillator with $\nu_{\mathrm{osc}} = 103$ GHz (power 0.5 mW) has been achieved [9]; the miniband width was 120 meV. Other materials such as InGaAs/AlAs [10] should allow to develop oscillators for still higher frequencies. The superlattice can either be integrated into a planar circuit or into a waveguide resonator [11].

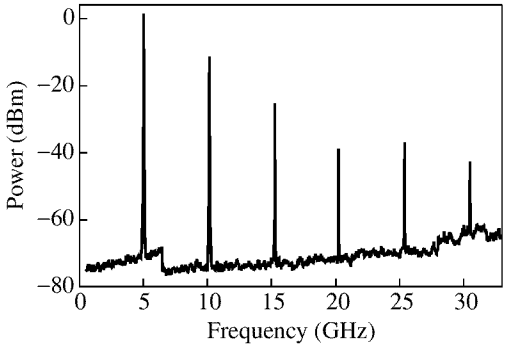

Fig. 5. Emission spectrum of the superlattice oscillator.

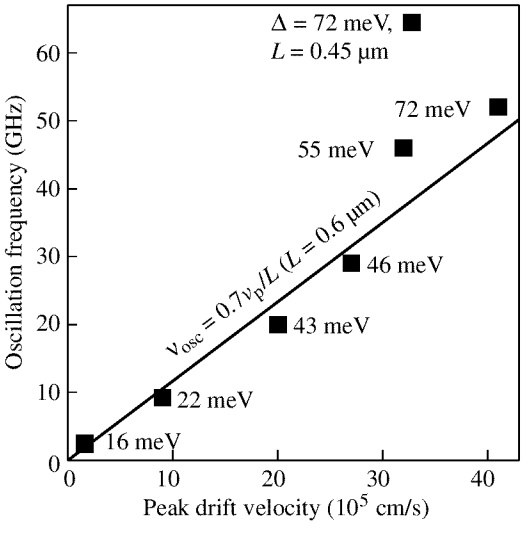

Fig. 6. Superlattice oscillator frequency for superlattices with different Δ.

3 Superlattice detector and frequency multiplier for microwaves

A microwave field influences the current through a superlattice according to the current-voltage characteristic leading to both a direct-current reduction [12] as well as generation of radiation at higher harmonics. Frequency multiplication up to the submillimeter frequency range (320 GHz) has been demonstrated [13, 14].

4 Superlattice detector and autocorrelator for THz radiation

A THz field can directly interact with a blochoscillating electron leading to a modulation of the Bloch frequency according to [14, 15]

$$\omega_B(t) = \frac{ea}{\hbar} E_s + \frac{ea}{\hbar} \hat{E}_\omega \cos(\omega t) \tag{3}$$

where $\hat{E}_\omega$ is the amplitude and ω the angular frequency of the THz field. The modulation leads to a reduction of the drift velocity [14, 15, 16, 17]. Accordingly, the current through a superlattice is reduced during THz irradiation. The response, i.e. the current reduction,

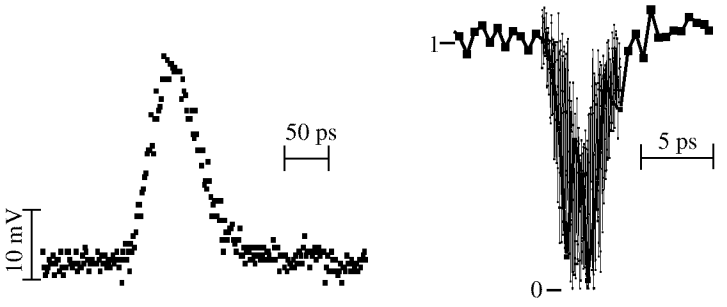

Fig. 7. Signal (left) and autocorrelation signal (right) for 4.3 THz radiation.

is proportional to the power of the radiation. The detection is illustrated in Fig. 7, which shows the response of a superlattice mesa, mounted in a corner cube antenna, on picosecond pulses of the FELIX free electron laser in Rijnhuizen (The Netherlands) [16]. The time resolution (50 ps) was determined by the registering sampling oscilloscope.

The superlattice acts as linear detector over many orders of magnitude of the power of the high-frequency field. At very strong irradiation, the current through the superlattice is almost completely suppressed [15, 16, 17]. This nonlinearity allows to perform autocorrelation experiments. In a first experiment [16] it has been demonstrated that the autocorrelator is able to resolve the 3 ps pulses of the FELIX laser (Fig. 7). The intrinsic time resolution of the detector and the autocorrelator is determined by the intraminiband relaxation time (10^{-13} s).

5 Conclusion

Wide-miniband semiconductor superlattice devices (at room temperature) can be used for generation, detection and frequency multiplication of microwave radiation up to frequencies above 100 GHz and, furthermore, for detection and autocorrelation of radiation at frequencies above 1 THz.

References

[1] L. Esaki und R. Tsu, *IBM J. Res. Dev.* **14**, 61 (1979).

[2] F. Bloch, *Z. Physik* **52**, 555 (1928); C. Zener, *Proc. Roy. Soc. London Ser. A* **145**, 523 (1934).

[3] A. Sibille, J. F. Palmier, H. Wang, J. C. Esnault and F. Mollot, *Appl. Phys. Lett.* **56**, 256 (1990); A. Sibille, J. F. Palmier, H. Wang, and F. Mollot, *Phys. Rev. Lett.* **64**, 52 (1990); M. Hadjazi, A. Sibille, J. F. Palmier, and F. Mollot, *Electron. Lett.* **27**, 1101 (1991).

[4] E. Schomburg, T. Blomeier, K. Hofbeck, J. Grenzer, S. Brandl, I. Lingott, A. A. Ignatov, K. F. Renk, D. G. Pavel'ev, Yu. Koschurinov, B. Ya. Melzer, V. Ustinov, S. Ivanov, A. Zhukov and P. S. Kop'ev, *Phys. Rev. B* **58**, 4035 (1998).

[5] K. Hofbeck, J. Grenzer, E. Schomburg, A. A. Ignatov, K. F. Renk, D. G. Pavel' ev, Yu. Koschurinov, B. Melzer, S. Ivanov, S. Schaposchnikov and P. S. Kop'ev, *Phys. Lett. A* **218**, 349 (1996).

[6] E. Schomburg, K. Hofbeck, J. Grenzer, T. Blomeier, A. A. Ignatov, K. F. Renk, D. G. Pavel'ev, Yu. Koschurinov, V. Ustinov, A. Zhukov, S. Ivanov and P. S. Kop'ev, *Appl. Phys. Lett.* **71**, 401 (1997).

[7] K. Hofbeck, E. Schomburg, J. Grenzer, K. F. Renk, D. G. Pavel'ev, Yu. Koschurinov, B. Melzer, S. Ivanov and P. S. Kop'ev, *IEEE Microw. Guid. Wave Lett.* **8**, 427 (1998).

[8] E. Schomburg, S. Brandl, K. Hofbeck, T. Blomeier, J. Grenzer, A. A. Ignatov, K. F. Renk, D. G. Pavel'ev, Yu. Koschurinov, V. Ustinov, A. Zhukov, A. Kovsch, S. Ivanov and P. S. Kop'ev, *Appl. Phys. Lett.* **72**, 1498 (1998).

[9] E. Schomburg, M. Henini, J. M. Chamberlain, D. P. Steenson, S. Brandl, K. Hofbeck, K. F. Renk and W. Wegscheider, *Appl. Phys. Lett.* **74** (1999).

[10] S. Brandl, E. Schomburg, R. Scheuerer, K. Hofbeck, J. Grenzer, K. F. Renk, D. G. Pavel'ev, Yu. Koschurinov, A. Zhukov, A. Kovsch, V. Ustinov and P. S. Kop'ev, *Appl. Phys. Lett.* **73**, 3117 (1998).

[11] J. Grenzer, A. A. Ignatov, E. Schomburg, K. F. Renk, D. G. Pavel'ev, Yu. Koschurinov, B. Melzer, S. Ivanov, S. Schaposchnikov and P. S. Kop'ev, *Ann. Physik* **4**, 184 (1995).

[12] E. Schomburg, A. A. Ignatov, J. Grenzer, K. F. Renk, D. G. Pavel'ev, Yu. Koschurinov, B. Ja. Melzer, S. Ivanov, S. Schaposchnikov and P. S. Kop'ev, *Appl. Phys. Lett.* **68**, 1096 (1996).

[13] E. Schomburg, J. Grenzer, K. Hofbeck, C. Dummer, S. Winnerl, A. A. Ignatov, K. F. Renk, D. G. Pavel'ev, Yu. Koschurinov, B. Melzer, S. Ivanov, V. Ustinov and P. S. Kop'ev, *IEEE J. Sel. Top. Quantum Electron.* **2**, 724 (1996).

[14] A. A. Ignatov, K. F. Renk and E. P. Dodin, *Phys. Rev. Lett.* **70**, 1996 (1993).

[15] A. A. Ignatov, E. Schomburg, J. Grenzer, K. F. Renk and E. P. Dodin, *Z. Phys. B* **98**, 187 (1995).

[16] S. Winnerl, E. Schomburg, J. Grenzer, H.-J. Regl, A. A. Ignatov, A. D. Semenov and K. F. Renk, *Phys. Rev. B* **56**, 10303 (1997).

[17] A. A. Ignatov, E. Schomburg, K. F. Renk, W. Schatz, J. F. Palmier and F. Mollot, *Ann. Physik* **3**, 137 (1994).

[18] S. Winnerl, W. Seiwerth, E. Schomburg, J. Grenzer, K. F. Renk, C. J. G. M. Langerak, A. F. G. van der Meer, D. G. Pavel'ev, Yu. Koschurinov, A. A. Ignatov, B. Melzer, V. Ustinov, S. Ivanov and P. S. Kop'ev, *Appl. Phys. Lett.* **73**, 2983 (1998); S. Winnerl, S. Pesahl, E. Schomburg, J. Grenzer, K. F. Renk, H. P. M. Pellemans, A. F. G. van der Meer, D. G. Pavel'ev, Yu. Koschurinov, A. A. Ignatov, B. Melzer, V. Ustinov, S. Ivanov, P. S. Kop'ev, *Superlattices Microstruct.* **25**, 57 (1999).